JOP. J Pancreas (Online) 2007; 8(2):156-165.

REVIEW

Optical Coherence Tomography for Investigation of the Pancreatico-Biliary System: Still Experimental?

Pier Alberto Testoni, Benedetto Mangiavillano, Alberto Mariani

Department of Gastroenterology and Gastrointestinal Endoscopy, IRCCS Vita-Salute San Raffaele University, San Raffaele Hospital Scientific Institute. Milan, Italy

Optical coherence tomography (OCT) is an optical imaging modality introduced in 1991 [1] that performs high-resolution, cross-sectional, subsurface tomographic imaging of the internal microstructure in materials and biologic systems by measuring backscattered or backreflected infrared light.

The physical principle of OCT is similar to that of B-mode ultrasound imaging, except that the intensity of infrared light, rather than sound waves, is measured. Wavelenghts of the infrared light used in OCT are one to two orders of magnitude higher than ultrasound wavelenght, so OCT technology can yield a lateral and axial spatial resolution of about 10 micron, which is 10- to 25-fold better than that of available high-frequency ultrasound imaging. The spatial resolution of OCT images is nearly equivalent to that of histologic sections. The depth of penetration of OCT imaging is approximately 1-3 mm, depending upon tissue structure, depth of focus of the probe used, and pressure applied to the tissue surface. Although the progressive increase in ultrasound resolution is accompanied by a corresponding decease in depth of penetration, a similar trade-off between resolution and depth of penetration does not occur in OCT imaging. In contrast to magnification endoscopy, OCT has depth.

Several *in vitro* studies demonstrated the feasibility of OCT in the gastrointestinal (GI) tract: in these studies the GI tract wall was identified as a multiple layer structure chraracterized by a sequence of hyper- and hypo-reflective layers, with a variable homogenicity of the back-scattered signal [2, 3, 4]. Neoplastic and normal tissue also showed different light backscattering patterns [5]. However, the optical properties of nonliving tissues are different from tissue *in vivo*.

Subsequent studies were therefore performed in *ex-vivo* tissue specimens and aimed at comparing OCT imaging with histology, to assess the realiability of the OCT technique to identify and recognize the GI wall structure. OCT was shown to clearly differentiate the layers' structure of the GI wall [6].

In the last decade, OCT technology has evolved from an experimental laboratory tool to a new diagnostic imaging modality with a wide spectrum of clinical applications in medical practice, including the gastrointestinal tract and pancreatico-biliary ductal system.

Technical OCT Principles of Operation

OCT devices use a low-power infrared light with a wavelenght ranging from 750 to 1300 nm in which the only limiting factor is the scattering of light. Scattering occurs when the light interacts with tissue surface and the image formation depends upon the difference in optical backscattering properties of the tissue.

OCT images are generated from measuring the echo time delay and the intensity of

backscattered light. Because the velocity of light is extremely high, optical echoes cannot be measured by direct electronic detection, but by means of a low-coherence interferometry that measures the interference of two incident light beams that are derived from a single source of low-coherence light. Low-coherence light can be generated by compact superluminescent semiconductor diodes or other sources, such as solid-state lasers.

In the low-coherence interferometry the light reflected or backscattered from inside the specimen is measured by correlating with light that has traveled a known reference path. One interferometer arm contains a modular probe that focuses and scans the light onto the tissue sample, also collecting the backscattered light; the second interferometer arm is a reference path with a translating mirror or scanning delay line [7].

Lights reflected from the specimen and reference beam are combined at a detector, and the interference between the two beams is measured. Optical interference between the light from the sample and reference path occurs only when the distance traveled by the light in both paths matches to within the coherence length of the light [8].

The coherence length of the light source, which is inversely proportional to its spectral bandwidth, determines the axial or depth resolution of OCT: the shorter the coherence length of the light source, the better is the in-depth spatial resolution. The spatial width of the scanning beam determines the lateral or transverse resolution. The image penetration depth is determined by the absorption and scattering properties of the sample surface.

In OCT, two-dimensional cross-sectional images of tissue microstructure are constructed by scanning the optical beam and performing multiple axial measurements of backscattered light at different transverse positions. The resulting data set is a two-dimensional array that represents the displayed as a grey-scale or false-color image.

Three types of scanning patterns are available for OCT imaging: radial [9, 10, 11], longitudinal [12, 13], and transverse [14]. The radial-scan probe directs the OCT beam radially, giving images that are displayed in a "radar-like", circular plot. Radial scanning can easily image large areas of tissue by moving the probe forth and back over the tissue surface and has the highest definition when the probe is inserted within a small diameter lumen, because the OCT images become progressively coarser when a large-diameter lumen is scanned, due to the progressive increase of pixel spacing with increasing the distance between the probe and the tissue. The linear and transverse probes scan the longitudinal and transverse positions of the OCT beam at a fixed angle, generating rectangular images of longitudinal and transverse planes at a given angle with respect to the probe. Linear scanning has the advantage that pixel spacing in the transverse direction is uniform and can better image a definite area of the scanned tissue, expecially in presence of large-diameter and non-circular lumens, where maintaining constant distance from the probe to the surface over the entire circumferential scan may be impossible. Transverse scanning modality provides a better depth of field. Depth of field is the range of distances from the probe over which optimal resolution of scaninng can be obtained; current OCT scans permit imaging depths of up to 2-3 mm in tissues, by using probes with different focuses.

OCT Technique for the Pancreatico-Biliary Ductal System Investigation

OCT imaging from the GI tract can be done in humans by using narrow-diameter, catheter-based probes [15]. The probe is deteachable from the OCT main unit, making it reprocessable between procedures.

The probe can be inserted through the accessory channel of a side-view endoscope, inside a standard transparent ERCP catheter, for investigating the pancreatico-biliary ductal system (Figure 1). The possibility to introduce the OCT probe into the pancreatico-biliary ductal system permits to investigate in detail the epithelial layers of the ductal system and sphincter of Oddi. OCT scanning can be done either keeping the OCT probe in the ERCP

catherer or leaving it in the duct outside the catheter (Figure 2).
From a clinical point of view, OCT imaging of the pancreatic and biliary ductal system could improve the diagnostic accuracy for ductal epithelial changes and the differential diagnosis between neoplastic and non-neoplastic lesions, since in several conditions X-ray morphology obtained by ERCP and other imaging techniques may be non-diagnostic, and the sensitivity of intraductal brush cytology during ERCP procedures is highly variable.
In our studies a near-focus OCT probe (Pentax, Lightlab Imaging, Westford, MA, USA) was used, with a penetration depth of about 1 mm and a resolution of approximately 10 μm. The probe operates at 1.2-1.4 μm center wavelength (nominal value: 1.3 μm), with a scan frequency ranging from 1,000 to 4,000 kHz (nominal value: 3,125 kHz). Radial and longitudinal scanning resolutions have an operating range in tissue of 15-20 μm (nominal value: 18 μm), and 21-27 μm (nominal value: 24 μm) respectively. Infrared light is delivered to the imaging site through a single optical fiber 0.006-inch diameter. OCT probe is assembled in a catheter with an outer diameter of 1.2 mm, The catheter-based probe consists of a rotating probe encased in a transparent outer sheath which remains stationary while the rotating probe has a pull-back movement of 1 mm/second, with an acquisition rate of 10 frames per second. By this technique a segment of tissue 5.5 cm long can be filmed over a 55-second period.

Experimental Investigation by OCT of the Pancreatico-Biliary Ductal System

Normal Pancreatico-Biliary Ductal System

Visualization of the normal epithelium of the main pancreatic duct has been obtained *post-mortem* [16] and *ex-vivo* in humans [17, 18], while *in-vivo* it comes from one study in animals [19]. Normal biliary ductal system has been investigated in humans, *ex vivo* in a study [17], *post-mortem* [16], and *in-vivo* in animals and human being [19, 20, 21].

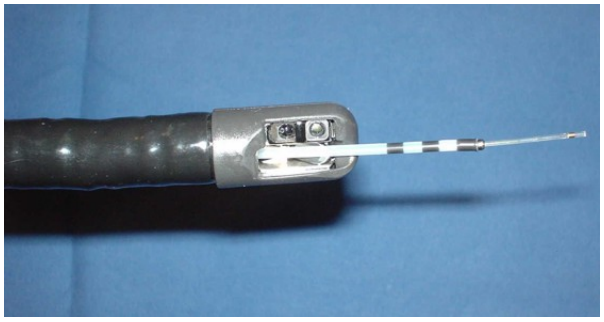

Figure 1. The duodenoscope with OCT mid-probe inside the ERCP catheter.

Tearney *et al*. in 1998 [16] published the first data in literature about the use of the OCT in the pancreato-biliary system, in a *post-mortem* study in human beings. OCT images of the common bile duct (CBD) wall were able to identify the layered structure and resolve the submucosa-muscularis and muscularis-adventitia boundaries. Differentiation of the submucosa, muscularis and adventitial layers was made possible by visualization of the different back-scattering characteristics within each layer. The adventitial layer seemed to have a lower and more irregular back-scattering intensity than the submucosa or muscularis. This irregular back-scattering pattern is most likely due to the presence of adipose tissue into the adventitial layer. High-resolution OCT imaging enabled tissue microstructure, such as secretions within individual glands, and cross-sectional imaging of islets Langherans cells to be visualized. The pancreatic duct,

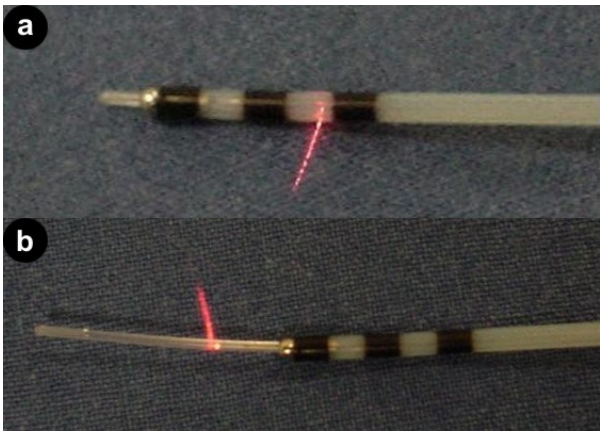

Figure 2. OCT probe inside (**a.**) and outside (**b**.) the ERCP catheter.

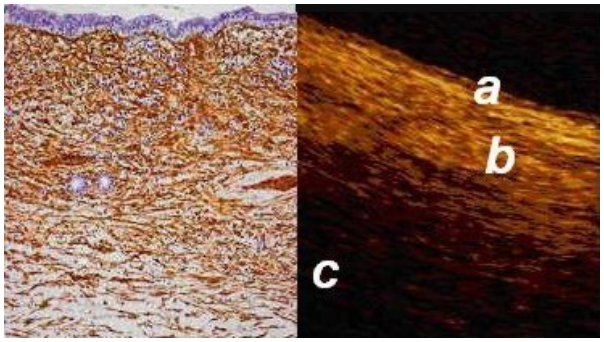

Figure 3. Magnification of an OCT image from the normal common bile duct wall, compared with histology. From the surface of the duct, up to a depth of 1 mm, the following layers are recognizable: a) the single layer of epithelial cells, approximately 0.04-0.06 mm thick, visible as a superficial, hypo-reflective band; b) the connective-muscular layer surrounding the epithelium, visible as a hyper-reflective layer approximately 0.34-0.48 mm thick; c) the connective layer visible as a hypo-reflective layer with longitudinal relatively hyper-reflective strips (smooth muscle fibers).

moreover, appeared as a highly back-scattering band near the lumen of the tissue. Pancreatic stroma was seen beneath the pancreatic duct.

Recently Singh *et al*. [19] published a study *in-vivo* in animals (dogs) on the OCT imaging of the pancreatic and biliary ductal system. OCT was able to identify the entire wall of the bile duct and some of the surrounding fibrous tissue but could not identify adjacent structures such as blood vessels. A thin, low-scattering, superficial layer could be discerned on the majority of the images, which was thought to represent the cuboidal epithelium. Nuclei or subcellular structures could not be identified. The lamina propria appeared to be a highly reflecting layer underneath the mucosal surface. The dense connective tissue underlying the lamina propria was imaged as linear layers of differing intensities. Peribiliary glands were seen as large open spaces with a single layer, signal-poor, epithelium. The pancreatic duct in dogs had a flat mucosal layer composed of cuboidal epithelium. OCT was able to image the wall of the pancreatic duct but not the surrounding parenchyma. The pancreatic duct on OCT images was homogeneous and moderately reflective.

In a study by our group [17], OCT imaging of main pancreatic duct, common bile duct and sphincter of Oddi normal structure has been shown to be able to provide features that were similar to those observed in the corresponding histological specimens in 80% of sections; the agreement between OCT and histology in the definition of normal wall was good (81.8%). OCT images identified three differentiated layers up to a depth of about 1 mm. From the surface of the duct, it was possible to recognize an inner hypo-reflective layer corresponding to the single layer of epithelial cells close to the lumen, an intermediate homogeneous hyper-reflective layer corresponding to the fibro-muscular layer surrounding the epithelium, and an outer, less definite, hypo-reflective layer corresponding to the smooth muscular structure within a connective tissue in the common bile duct and at the level of the sphincter of Oddi, and connective-acinar structure in the main pancreatic duct (Figures 3, 4, 5).

The inner, hypo-reflective layer showed a mean thickness of 0.05 mm (range 0.04-0.08 mm) and a homogeneneous back-scattering of

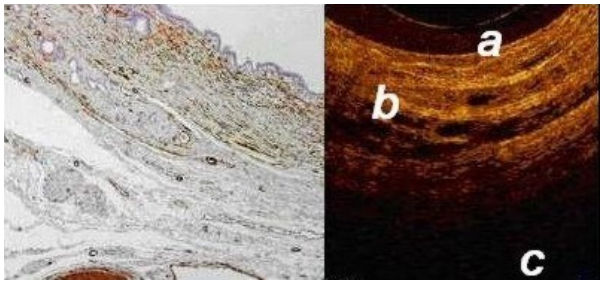

Figure 4. Magnification of an OCT image from the normal sphincter of Oddi wall, compared with histology. From the surface of the duct, up to a depth of 1 mm, the following layers are recognizable: a) the single layer of epithelial cells, approximately 0.04-0.08 mm thick, visible as a superficial, hypo-reflective band; b) the connective-muscular layer surrounding the epithelium, visible as a hyper-reflective layer approximately 0.23-0.37 mm thick; c) the connective layer visible as a hypo-reflective layer with longitudinal relatively hyper-reflective strips (smooth muscle fibers). Within the intermediate and outer layer vessels are also recognizable, visualized as non-reflecting areas surrounded by an hypo-reflective endothelium. Margins between the intermediate and outer layer are poorly recognizable, due to the irregular distribution of connective and muscular structure.

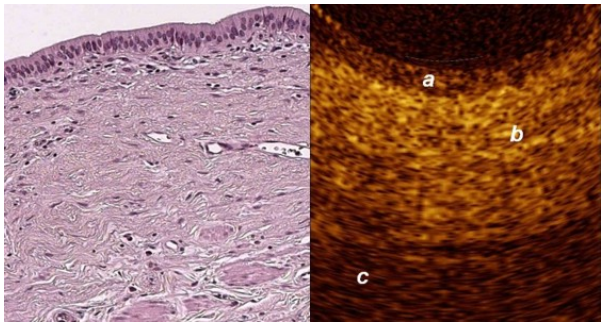

Figure 5. Magnification of an OCT image from the normal main pancreatic duct wall, compared with histology. From the surface of the duct, up to a depth of 1 mm, the following layers are recognizable: a) the single layer of epithelial cells, approximately 0.04-0.08 mm thick, visible as a superficial, hypo-reflective band; b) the connective-fibro-muscular layer surrounding the epithelium, visible as a hyper-reflective layer approximately 0.36-0.56 mm thick; c) the connective and acinar structure close to the ductal wall epithelium, visible as a hypo-reflective layer.

the signal in all the imaged sites; thickness, surface regularity, and reflectance degree of this layer did not substantially differ in the common bile duct, main pancreatic duct, and sphincter of Oddi. The intermediate layer showed a mean thickness of 0.41 mm (range: 0.34-0.48 mm) in the common bile duct, 0.42 mm (range: 0.36-0.56 mm) in the main pancreatic duct, and 0.29 mm (range: 0.23-0.37 mm) in the sphincter of Oddi. The layer thickness was substantially similar in the ducts, while appeared reduced by 25% at the level of the sphincter of Oddi. The layer appeared hyper-reflective when compared with the inner and outer layers and the reflectance degree did not change in all the imaged sites. Within the context of the intermediate layer, tiny, multiple, non-reflective areas were recognizable in the main pancreatic duct and at the level of sphincter of Oddi. The outer layer appeared recognizable until a depth of about 1 mm from the lumen and was hypo-reflective in all the imaged sites. Multiple, hyper-reflective, longitudinal strips were recognizable at the level of common bile duct and sphincter of Oddi. These longitudinal strips were more pronounced and hyper-reflective in the sphincter of Oddi, so the layer appeared at this level less hypo-reflective than in the common bile duct.

The three different layers showed a linear, regular surface and each layer had a homogeneous back-scattered signal in every frame; however, the differentiation between the intermediate and outer layer appeared more difficult than between the inner and intermediate layer. The thickness of the inner and intermediate layers measured by OCT was similar to those measured by histology; the muscular and connective-acinar structure was visible until the working depth of penetration into the tissue of the near-focus probe (about 1 mm).

Smooth muscle structure appeared at OCT scanning as hyper-reflective, longitudinal strips within a context of hypo-reflective tissue and were particularly recognizable at the level of sphincter of Oddi. Veins, arteries and secondary pancreatic ducts were also identifiable by OCT, characterized by hypo- or non-reflective, well-delimited areas (Figure 6).

The images acquired in this study provided information on tissue architectural morphology that could have only previously be obtained with conventional biopsy. These

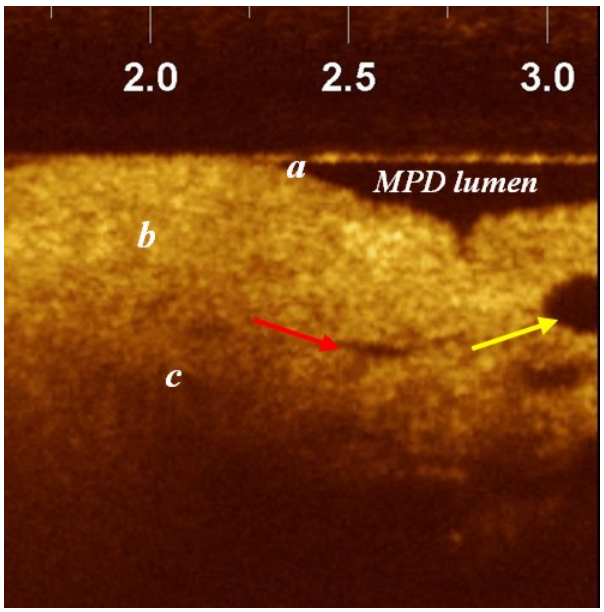

Figure 6. OCT image from the normal main pancreatic duct wall visualized by linear array OCT: a portion of an accessory duct is visible close to the pancreatic duct (yellow arrow) as a non-reflective, well-delimited area, with larger diameter than observed for blood vessels (red arrow). From the lumen to the depth is it possible to recognize: a, epithelium; b, fibro- connectival tissue; c. acinar tissue.

results suggest that OCT could become a powerful imaging technology, enabling high-resolution diagnostic images to be obtained from the pancreato-biliary system during a diagnostic ERCP procedure.
Although OCT images were obtained from surgical specimens, the early evaluation (within one hour from pancreatic resection) of ductal OCT-imaged morphology was not likely to have been influenced by artifacts induced by autolytic tissue degradation occurring in autopsy specimens, as reported in previous studies [12, 17, 18]. The data obtained *ex vivo* from this study can therefore be considered useful for *in vivo* evaluation too.

Pathological Pancreatico-Biliary Ductal System

Pathological pancreatic ductal system has been investigated by our group in humans in two *ex vivo* studies [12, 18, 22] performed on multiple surgical pancreatic specimens obtained from patients with pancreatic head adenocarcinoma.
In chronic inflammatory changes involving the main pancreatic duct OCT still showed a conserved three-layer architecture. However, the inner, hypo-reflective layer appeared slightly larger than normal (0.07-0.24 mm), and the intermediate layer appeared more hyper-reflective than in normal tissue; this is probably because of the dense mononuclear cell infiltrate. The back-scattered signal was heterogeneous with marked hypo- or hyper-reflectance in some sections.
The agreement between OCT and histology in the definition of main pancreatic duct (MPD) chronic inflammatory changes was poor (27.7%).
The OCT pattern in presence of dysplasia of the main pancreatic duct epithelium was characterized by an inner layer markedly thickened (0.49 mm), strongly hipo-reflective and heterogeneous; this OCT finding is probably due to the initial structural disorganization (increased mitosis and altered nucleus/cytoplasm ratio). The surface between the inner and intermediate layers appeared irregular. As in chronic inflammatory tissue, dysplasia too gave strong hyper-reflectance of the intermediate layer, particularly in the part closest to the inner layer. The outer layer did not differ from other non-malignant conditions and appeared homogeneously hypo-reflective.
However, in chronic pancreatitis and dysplasia only in 62% of cases OCT and histology were concordant. The K statistic used to assess agreement between the two procedures was equal to 0.059 for non neoplastic MPD wall appearance.
Overall, normal wall structure and chronic inflammatory or low-grade dysplastic changes cannot be distinguished in 38% of the sections because the architecture of the layers and surface light reflection did not show a characteristic OCT pattern.
In all sections with histologically proven adenocarcinoma OCT showed a totally subverted MPD wall architecture. The three layers of the ductal wall and their linear, regular surface, normally giving a homogeneous back-scattered signal, were not recognizable. The margins between the connective-fibro-muscular layer and acinar tissue were unidentifiable. The back-scattering of the signal appeared strongly heterogeneous, with minute, multiple, non-reflective areas in the disorganized pancreatic microstructure. In 100% of sections with adenocarcinoma OCT and histology were concordant. A totally subverted wall architecture was also observed by OCT in presence of neoplastic tissue within the common bile duct [21].
Figure 7 shows magnified OCT images from sections of main pancreatic duct with normal tissue, chronic pancreatitis, low-grade dysplasia, and adenocarcinoma.

Clinical Application of OCT in the Pancreatico-Biliary Ductal System

Segmental strictures of the MPD may in fact be difficult to investigate, particularly when they are in the middle and tail of the gland. In these cases a definite diagnosis can be achieved only by cytology, either by intraductal brushing or fine needle aspiration

biopsy (FNAB). The diagnostic accuracy of brush cytology tends to be low [23, 24, 25], while FNAB, though it offers satisfactory accuracy, is an invasive technique and usually requires EUS as an additional procedure. OCT could therefore be a useful, not excessively invasive technique for investigating in detail the MPD wall structure in patients with segmental stricture, since the probe can be inserted into the pancreatic duct and segmental strictures through a standard transparent ERCP catheter. Repeated frames can be taken by the pull-back technique in a few minutes, giving a large number of radial and longitudinal images. The transparent surface of the ERCP catheter did not substantially affect the OCT diagnostic capacity, compared with images obtained keeping the probe outside the catheter.

The MPD has been investigated by OCT during ERCP procedures by our group in a series of 12 consecutive patients with documented or suspected MPD stricture at a previous CTscan or MRCP; all patients underwent endoscopic ultrasonography before ERCP [22]. OCT recognized a differentiated three-layer architecture in all cases with normal MPD or chronic pancreatitis, while in all the neoplastic lesions the layer architecture appeared totally subverted, with heterogeneous back-scattering of the signal. OCT was able to distinguish a non-neoplastic from a neoplastic MPD wall in all cases and was superior to brush cytology; OCT gave 100% accuracy for detection of neoplastic tissue compared with 66.7% for brush cytology. The presence or absence of a recognizable three-layer architecture within the MPD wall, derived from the different back-scattered signals from each layer, was confirmed as a reliable OCT parameter for distinguishing non-neoplastic from neoplastic tissue, as already documented in previous experimental studies. Despite the superiority of the OCT to distinguish a non-neoplastic from a neoplastic MPD stricture, the technique appeared substantially unable to discriminate between a normal MPD structure and other benign lesions of the MPD. The catheter sheet made it difficult to examine the inner hypo-reflective layer of the MPD wall, corresponding to the single layer of epithelial cells of the MPD surface, particularly when the MPD diameter was small. This occurred particularly when OCT frames were obtained inside the strictures, as the superficial epithelial layer was compressed by the ERCP catheter. However, the diagnostic capacity of the technique was not substantially affected, since the differential diagnosis between non-neoplastic and neoplastic lesions was based on identification of the layer architecture (Figure 8).

OCT scanning performed within ERCP has been also useful in identifying neoplastic lesions at early stages involving the common bile duct, missed by cytology and X-ray imaging (Figure 9).

OCT imaging of the biliary ductal system has been done *in-vivo* in two previous ERCP-

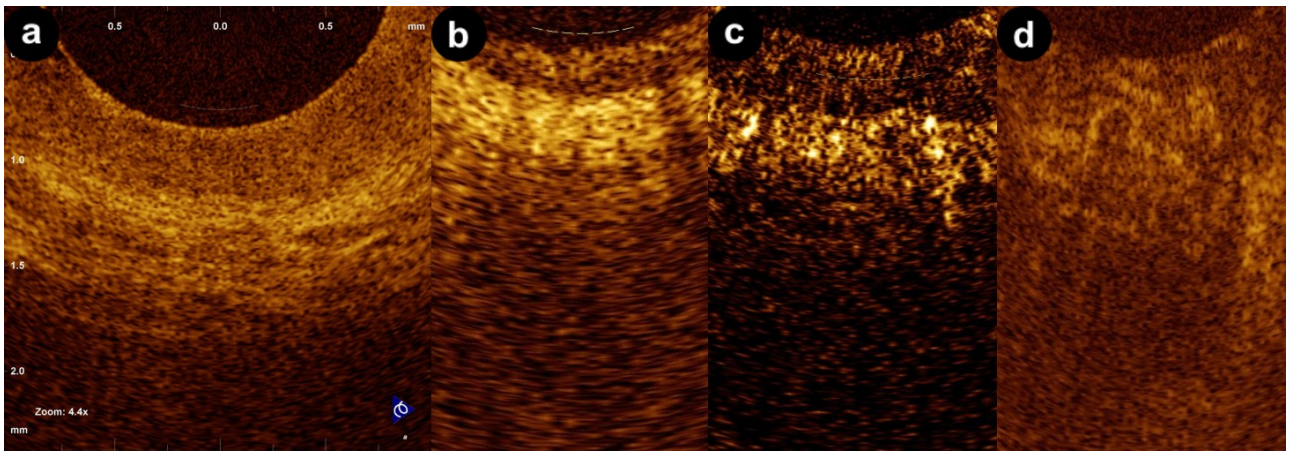

Figure 7. Magnified OCT images from sections with either normal (**a.**), tumor-associated chronic inflammatory (**b.**), low-grade dysplasia (**c.**), and adenocarcinoma (**d.**) tissue.

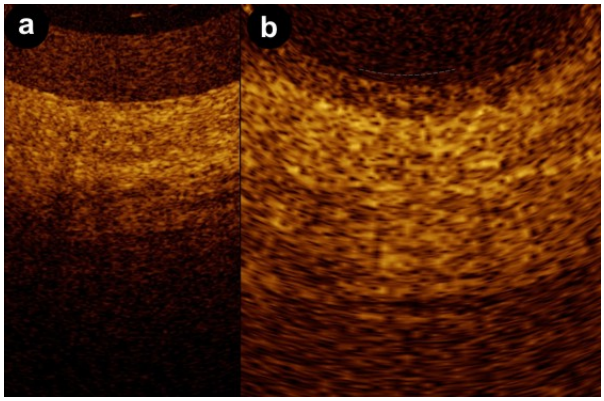

Figure 8. Intraductal magnified OCT images of a pancreatic duct outside (**a.**) and inside (**b.**) an ERCP catheter.

based studies [20, 21]. The first OCT evaluation of the biliary ductal system was done in four cases by Seitz *et al*. [21], who demonstrated the feasibility of the technique in patients with biliary pathology and obtained interpretable images. The connective tissue layer and the underlying retroperitoneal tissue, with a reduced light back-scattering, were clearly demonstrated, toghether with the intramural glands, visualized as non-reflective areas. The second *in-vivo* study by Poneros *et al*. [20] showed the technique was feasible during a convenctional ERCP in 5 patients and recognized the normal OCT pattern, compared to histology, of both intra- and extra-hepatic biliary tree; OCT pattern of epithelial and subepithelial structures, including peribiliary glands, vascular and hepatic structure were described. The Authors also reported the OCT pattern of inflamed biliary ducts and cholangiocarcinoma. The normal bile duct was characterized by a layered structure similar to that observed by Authors in *ex-vivo* images. The superficial cuboidal epithelium was observed as a thin, hypo-reflective layer overlying an hiper-reflective submucosa and a weakly-reflective serosa. The inflammed bile duct was described as heterogeneously-reflective submucosal layer with dilated peribiliary glands. OCT pattern of cholangiocarcinoma was characterized by a villous morphology, with an underlying fibrous stroma clearly differentiable from the non-neoplastic tissue.

Future of the OCT in the Pancreatic-Biliary Ductal System

Recently, a new linear-array OCT (LOCT) has been proposed in Europe for experimental use only, with an higher resolution rate (21-27 μm) than the radial one (ROCT), a same frame acquisition and penetration depth. Up to now, LOCT is allowed to be tested only in animals and surgical specimens. In a pilot study we evaluated the accuracy of LOCT, compared with ROCT, in the recognition of the normal CBD layers' structure in a series of surgical specimens from patients who had undergone pancreatic head resection for pancreatic cancer not involving the biliary tree. Images obtained by LOCT and ROCT were compared with the corresponding histologic features (Figures 10). LOCT images appeared superior to those obtained by ROCT for the recognition of CBD wall microstructure, particularly at the level of the intermediate fibro-connectival submucosal layer. The possibility to recognize in detail the microstructure of the connective and muscular layer could be useful in the

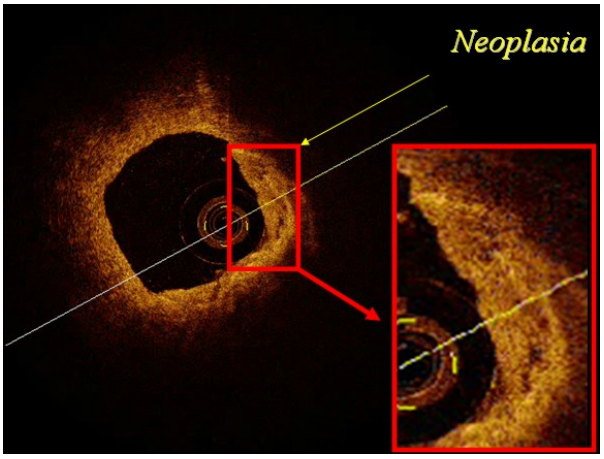

Figure 9. Adenocarcinoma of the common bile duct at early stage detected by OCT during ERCP. Whithin a normal tissue, OCT recognizes a delimited area showing a subverted wall architecture, with loss of the ductal layers and unidentifiable connective and muscular layer. The three layers and their linear and regular surface, normally giving an homogeneous back-scattered signal, are not recognizable. This OCT image has an heterogeneous back-scattered signal with minute, multiple, non-reflective areas (necrotic areas) in the disorganized CBD microstructure.

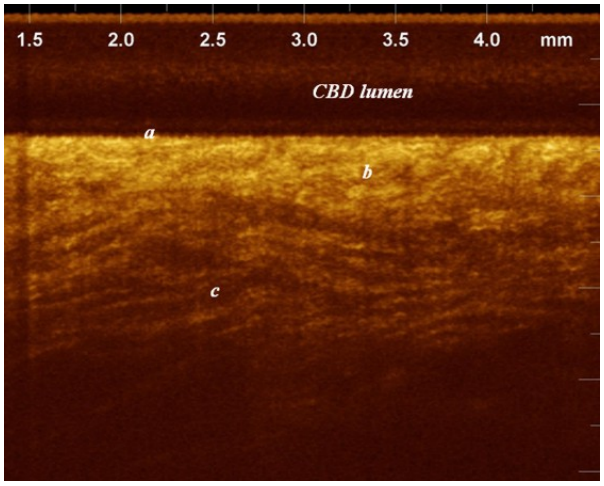

Figure 10. Magnification of an image of a normal CBD wall acquired with the linear optical coherence tomography (LOCT). From the lumen to the depth it is possible to recognize: a, epithelium; b, fibro-connectival tissue; c, muscular fibers.

diagnosis of inflammatory strictures, histologically characterized by an increase of both connective fibers and thickness of the connective layer. This characteristic histological pattern could be recognized by LOCT scan, by measuring the connective layer thickness and infrared light back-scattering reflectance, that might be extremely hyper-reflective because of the increased number of hypertrophic connective fibers induced by fibrosis and lymphocytic infiltrate.

Conclusions

OCT appears a promising technique for real-time, high-resolution, cross-sectional imaging of the pancreatico-biliary ductal system during routine endoscopic procedures. It has been shown to be a highly sensitive and specific means of identifying neoplastic tissue and distinguishing between non-neoplastic and neoplastic tissue. To date, the technique has been documented to be particularly useful in the investigation of pancreatico-biliary ductal system when strictures of unknown etiology are identified during an ERCP procedure, being its diagnostic accuracy higher than reported for intraductal brush cytology. LOCT may further improve the diagnostic capacity of the technique. Its capacity to recognize the presence of fibrotic tissue within the intermediate connective-muscular layer of the ducts may allow to identify inflammatory lesions. Moreover, the LOCT easy recognition of vessels could also permit, in association with the Doppler technology, to improve the diagnostic accuracy in presence of undefined lesions.

Keywords Biliary Tract; Cholangio-pancreatography, Endoscopic Retrograde Pancreatic Ducts; Sphincter of Oddi; Tomography, Optical Coherence

Abbreviations CBD: common bile duct; FNAB: fine needle aspiration biopsy; LOCT: linear-array optical coherence tomography; MPD: main pancreatic duct; OCT: optical coherence tomography; ROCT: radial optical coherence tomography

Correspondence
Pier Alberto Testoni
Division of Gastroenterology and
Gastrointestinal Endoscopy
University Vita-Salute San Raffaele
IRCCS Scientific Institute San Raffaele
Via Olgettina, 60
20132 Milan
Italy
Phone: +39-02.2643.2756/2145/2744
Fax: +39-02.2643.3491
E-mail: testoni.pieralberto@hsr.it

Document URL: http://www.joplink.net/prev/200703/03.html

References

1. Huang D, Swanson EA, Lin CP, Schuman JS, Stinson WG, Chang W, et al. Optical coherence tomography. Science 1991; 254:1178-81. [PMID 1957169]

2. Tearney GJ, Brezinski ME, Southern JF, Bouma BE, Boppart SA, Fujimoto JG. Optical biopsy in human gastrointestinal tissue using optical coherence tomography. Am J Gastroenterol 1997; 92:1800-4. [PMID 9382040]

3. Kobayashi K, Izatt JA, Kulkarni MD, Willis J, Sivak MV Jr. High-resolution cross-sectional imaging of the gastrointestinal tract using optical coherence tomography: preliminary results. Gastrointest Endosc 1998; 47:515-23. [PMID 9647378]

4. Westphal V, Rollins AM, Willis J, Sivak MV, Izatt JA. Correlation of endoscopic optical coherence tomography with histology in the lower-GI tract. Gastrointest Endosc 2005; 61:537-46. [PMID 15812406]

5. Pitris C, Jesser C, Boppart SA, Stamper D, Brezinski ME, Fujimoto JG. Feasibility of optical coherence tomography for high-resolution imaging of human gastrointestinal tract malignancies. J Gastroenterol 2000; 35:87-92. [PMID 10680662]

6. Izatt JA, Kulkami MD, Wang HW, Kobayashi K, Sivak MV Jr. Optical coherence tomography and microscopy in gastrointestinal tissues. IEEE Journal of Selected Topics in Quantum Electronics 1996; 2:1017-28.

7. Fujimoto JG. Optical coherence tomography for ultrahigh resolution in vivo imaging. Nat Biotechnol 2003; 21:1361-7. [PMID 14595364]

8. Brezinski ME, Fujimoto JG. Optical coherence tomography: high-resolution imaging in non transparent tissue. IEEE Journal of Selected Topics in Quantum Electronics 1999; 5:1185-92.

9. Shen B, Zuccaro G Jr. Optical coherence tomography in the gastrointestinal tract. Gastrointest Endosc Clin N Am 2004; 14:555-71. [PMID 15261202]

10. Sivak MV Jr, Kobayashi K, Izatt JA, Rollins AM, Ung-Runyawee R, Chak A, et al. High-resolution endoscopic imaging of the GI tract using optical coherence tomography. Gastrointest Endosc 2000; 51:474-9. [PMID 10744825]

11. Das A, Sivak MV, Chak A, Wong RCK, Westphal V, Rollins AM, et al. High-resolution endoscopic imaging of the GI tract: a comparative study of optical coherence tomography versus high-frequency catheter probe EUS. Gastrointest Endosc 2001; 54:219-24. [PMID 11474394]

12. Testoni PA, Mangiavillano B, Albarello L, Arcidiacono PG, Mariani A, Masci E, Doglioni C. Optical coherence tomography to detect epithelial lesions of the main pancreatic duct: an ex vivo study. Am J Gastroenterol 2005; 100:2777-83. [PMID 16393235]

13. Bouma BE, Tearney GJ, Compton CC, Nishioka NS. High-resolution imaging of the human esophagus and stomach in vivo using optical coherence tomography. Gastrointest Endosc 2000; 51:467-74. [PMID 10744824]

14. Poneros JM, Brand S, Bouma BE, Tearney GJ, Compton CC, Nishioka NS. A diagnosis of specialized intestinal metaplasia by optical coherence tomography. Gastroenterology 2001; 120:7-12. [PMID 11208708]

15. Zuccaro G, Gladkova N, Vargo J, Feldchtein F, Zagaynova E, Conwell D, et al. Optical coherence tomography of the esophagus and proximal stomach in health and disease. Am J Gastroenterol 2001; 96:2633-9. [PMID 11569687]

16. Tearney GJ, Brezinski ME, Southern JF, Bouma BE, Boppart SA, Fujimoto JG. Optical biopsy in human pancreatobiliary tissue using optical coherence tomography. Dig Dis Sci 1998; 43:1193-9. [PMID 9635607]

17. Testoni PA, Mariani A, Mangiavillano B, Albarello L, Arcidiacono PG, Masci E, Doglioni C. Main pancreatic duct, common bile duct and sphincter of Oddi structure visualized by optical coherence tomography: An ex vivo study compared with histology. Dig Liv Dis 2006; 38:409-14. [PMID 16584931]

18. Testoni PA, Mangiavillano B, Albarello L, Mariani A, Arcidiacono PG, Masci E, Doglioni C. Optical coherence tomography compared with histology of the main pancreatic duct structure in normal and pathological conditions: an 'ex vivo study'. Dig Liv Dis 2006; 38:688-95. [PMID 16807151]

19. Singh P, Chak A, Willis JE, Rollins A, Sivak MV Jr. In vivo optical coherence tomography imaging of the pancreatic and biliary ductal system. Gastrointest Endosc 2005; 62:970-4. [PMID 16301046]

20. Poneros JM, Tearney GJ, Shiskov M, Kelsey PB, Lauwers GY, Nishioka NS, Bouma BE. Optical coherence tomography of the biliary tree during ERCP. Gastrointest Endosc 2002; 55:84-8. [PMID 11756925]

21. Seitz U, Freund J, Jaeckle S, Feldchtein F, Bohnacker S, Thonke F, et al. First in vivo optical coherence tomography in the human bile duct. Endoscopy 2001; 33:1018-21. [PMID 11740643]

22. Testoni PA, Mariani A, Mangiavillano B, Arcidiacono PG, Di Pietro S, Masci E. Intraductal optical coherence tomography for investigating main pancreatic duct strictures. Am J Gastroenterol 2006;101:1-6. [PMID 17100970]

23. Vandervoort J, Soetikno RM, Montes H, Lichtenstein DR, Van Dam J, Ruymann FW, et al. Accuracy and complications rate of brush cytology from bile duct versus pancreatic duct. Gastrointest Endosc 1999; 49:322-7. [PMID 10049415]

24. Pugliese V, Pujic N, Saccomanno S, Gatteschi B, Pera C, Aste H, et al. Pancreatic intraductal sampling during ERCP in patients with chronic pancreatitis and pancreatic cancer: cytologic studies and K-ras-2 codon 12 molecular analysis in 47 cases. Gastrointest Endosc 2001; 54:595-9. [PMID 11677475]

25. Basir Z, Pello N, Dayer AM, Shidham VB, Komorowski RA. Accuracy of cytologic interpretation of pancreatic neoplasms by fine needle aspiration and pancreatic duct brushings. Acta Cytol 2003;47:733-8. [PMID 14526670]